CDF/ANAL/JET/CDFR/959
Jul 30, 1990

Moment Analysis of Jet Fragmentation Function and Quark Gluon Separation in CDF Dijet and γ+jet Events

S. Kanda, S. Kim and K. Kondo
Institute of Physics
University of Tsukuba

Abstract

For the experimental distinction of two types of partons—quarks and gluons, a method based on Monte Carlo simulaions which incorpolate the color-fragmentation scheme such as String and Cluster models is proposed. A number of variables, including mechanical/electric moments, multiplicity, and EM fraction, are calculated for Monte Carlo (reference) jets. The resulting distributions of variables indicate that gluon jets are softer and broader than quark jets, reflecting the nature of the double color charge of the gluon. The moment analysis on the CDF dijet events shows that the CDF dijets are close to, but slightly softer and broader than, the MC gluon jets. The gluon fractions in the dijet and γ+jet events obtained by the CDF experiment are estimated by comparing the likelihood distributions for the reference and real data jets. In the jet transverse energy range of 10–30 GeV, the dijet data are shown to contain approximately 80% of gluon fraction, while the γ+jet data about 40% of gluon fraction. The gluon fraction in the CDF dijet sample decreases with E_t as expected from QCD. In addition, the γ+jet data agree with the gluon fraction determined from theoretical predictions and the expected π^0/γ ratio in the CDF photon candidates. Some discrepancies between the QCD predictions analyzed with current fragmentation models and the CDF results are also discussed.

The difference of the structure between the quark-initiated and gluon-initiated jets have been a subject which interested considerable number of authors[1−6]. In this letter, we discuss the possibility of separating the quark jets from the gluon jets. The ideal way to study the quark ancestors is to use the experimental data sets consisting of the pure ancestors. Since this is rather difficult at present, we resort in this letter to the Monte Carlo (MC) events based on the phenomenological models of fragmentation to get a clue to the problem. There are three kinds of well known fragmentation models; the independent fragmentation [7], the string fragmentation [8], and cluster fragmentation [9,10,11]. The independent fragmentation model is not appropriate for our purpose of differentiating a quark from a gluon jet, because this model has such fundamental problems [12,13] as energy non-conservation and absence of any specific model of the gluon fragmentation. We therefore use two Monte Carlo programs, Herwig [14] and Pythia [15,16], which are based on the cluster and string models respectively.

The CDF detector has been described in ref. [17]. In this analysis, only jets detected by the "central" detectors are used. In the 1.5 T magnetic field, there are two kinds of tracking chambers, the vertex time projection chambers (VTPC) and the central tracking chamber (CTC). The CTC covers $|\eta| < 1.2$, and the transverse momentum resolution is $\Delta p_t/p_t^2 = 0.001\ (\mathrm{GeV}/c)^{-1}$. Outside the tracking chambers, the central electromagnetic (CEM) and hadronic (CHA/WHA) calorimeters are arranged in projective towers of size $\delta\eta = 0.1$ by $\delta\phi = 15°$. The strip chambers (CES) are embedded in the CEM at a depth of six radiation lengths.

We choose the CDF dijet events from 1987 run as a gluon rich-sample, because the dominant dijet final state is gluon-gluon at the CDF energy. The integrated luminosity for dijet events used in the analysis is approximately 26 nb^{-1}. The data were clustered using the fixed-cone algorithm [18] with a radius of 0.7 unit in $R = \sqrt{d\eta^2 + d\phi^2}$. For the hardware $\sum E_t$ triggers with threshold values of 20, 25, 40, and 45 GeV, cuts in the off-line analysis were placed on central-central jets at 36, 48, 56, and 60 GeV respectively, after jet energy corrections to the calorimeter data are made. We require the energy centroid of the leading and the next to leading jets to be in the central region $0.1 \leq |\eta| \leq 0.7$, and to be within 20° of back-to-back in ϕ .

For the track association to a jet, we first boost the events to the longitudinal dijet center of mass system using the corrected 4-vectors of the jets. In this Lorentz transformation, the masses of all charged particles are assumed to be equal to the pion mass. In the dijet rest frame, a cone is formed around the jet axis. This cone is defined by a minimum pseudorapidity $\eta_\perp$ with respect to the jet axis. The tracks within the cone are selected as jet particles, but tracks with poor quality are removed by requiring three-dimensional reconstruction capability and other quality cuts such as impact parameter or delta-z cut [19]. For the 1987 data, we also exclude

these jets whose axis are in the region, $-24° \leq \phi \leq 35°$ and $188° \leq \phi \leq 247°$ (*Dead Region* $\pm$ 20°) because of the dead cells in the CTC.

For a quark-rich sample we used photon+jet events. Events were selected from the 1988-89 runs by requiring an isolated electromagnetic (EM) cluster and one jet in the opposite hemisphere ($\pm$ 25° in ϕ) in the central region. The photon identification is done in the following way. We require that sharing of the lateral shower energy between CEM towers to be consistent with that for a photon shower, and that the averaged chisquared value derived from CES shower profiles in wire and strip views, $\chi^2_{av} = 0.5 \times (\chi^2_{strip} + \chi^2_{wire})$, to be less than 4. Both strip and wire clusters are also required with approximately equal energies; $\frac{E_{strip}-E_{wire}}{E_{strip}+E_{wire}} < 0.2$. The fitted cluster centroids are further required to be well within the active region of the CES chamber. The hadronic-to-EM ratio of the energy in the cluster is required to be less than $0.055 + 0.045 \cdot E/100$. An isolation requirement $I = \frac{E_c-E_t}{E_t} \leq 0.15$ is also made. Here, E_t and E_c are the total transverse energy of the EM cluster, and that within a cone of radius $R = 0.7$ centered on the EM cluster, respectively. Finally we require existence of no track pointing at the towers in the cluster.

For each jet in the dijet rest frame, we define the z' axis along the jet direction, and the y' axis along the direction of $\mathbf{p} \times \hat{\mathbf{z}}'$, where $\mathbf{p}$ is the momentum of the proton and $\hat{\mathbf{z}}'$ is the unit vector along the z' axis.

Since the analysis is based on MC generators, we will describe how we produce MC samples for gluon and quark jets We first produce quark and gluon jets in QCD $2 \rightarrow 2$ processes at $\sqrt{s}$ =1.8 TeV by using event generators, Herwig and Pythia. We pick up only those processes in which final partons are purely quarks or gluons: Thus the q g $\rightarrow$ q g process is not used. The generated events are then processed through a detector simulation program which reproduces the CDF detectors realistically. Next we reconstruct events: The simulated events are clustered by one of the CDF jet finding algorithms, in which one uses a cone of a fixed radius to define a jet. We then select only dijet events according to the clustering algorithm. The events are further divided into four samples, depending on the jet transverse energy E_t; 10-20,20-30,30-40 and 40-50GeV. In each E_t range, 2000(quark)+2000(gluon) jets are finally produced. We shall call gluon and quark sets as "reference" sets.

Such observables as multiplicity, a jet angular width, etc., have been pointed out to show differences between quarks and gluons [1-3]. In this analysis, however, we do not try to find ad hoc variables which are more sensitive to the differences between the parton ancestors. Instead, we take a systematic approach of analyzing the momentum distribution (the fragmentation function) of charged particles in a jet by using a method of moment analysis. It is motivated by the fact that a function (the momentum distribution function in a jet in this case) of variables (the momenta of charged particles here) can generally be expressed by their moments as defined by the Mellin transformation. More terms of different orders reproduce the

function more precisely. We take about 30 variables in the present treatment.

The variables which we choose are mainly divided into two classes: one is the m-th power of the momentum, summed over all particles, which we call the "mechanical moment"; $\sum_{i=1}^{n}(p_{li}/M)^m$ and $\sum_{i=1}^{n}(p_{ti}/M)^m$, where the term $(P_i/M)^m$ represents the m-th power of the normalized momentum of the i-th charged particle, n is the total number of charged particles in a jet, and M is the jet invariant mass. The suffix l and t indicate the momentum components: longitudinal and transverse to the jet axis respectively. The other is the m-th power of the momentum multiplied by the electric charge of the particle and summed over all particles, which we call the "electric moment"; $\sum_{i=1}^{n} C_i(p_{li}/M)^m$ and $\sum_{i=1}^{n} C_i(p_{ti}/M)^m$, where C_i is charge of the i-th charged particle.

In this analysis, the moments are calculated in the jet rest frame which is obtained, as mentioned earlier, by the Lorentz transformation along the jet axis. The reason why we try this coordinate system is that the moment variables thus defined are Lorentz invariant and are expected to be less energy (mass in this system) dependent. In this treatment, however, a certain ambiguity is introduced for the definition of moments, because we usually have soft particles in the lab system about which we do not know whether they belong to the jet or to the underlying event. The soft components do not give substantial effects in the determination of the jet CM system, but they acquire large backward momenta by the Lorentz boost to the jet CM frame, giving non-trivial contributions to the values of moments. In order to remedy this flaw, we take sums only over particles whose momenta lie in a forward hemisphere of the jet CM momentum space.

The choice of variables to form a set is somewhat arbitrary. Here we take a variable set with integers, $m = -3, -2, -1, 0, 1, 2, 3, 4$, for powers of moments as shown in table 1. The negative power means that we deal with the inverse of the momentum instead of the momentum itself, and the 0-th power corresponds to the multiplicity of charged particles. By the uncertainty relation, the higher positive moments provide information about the inner part of the jet in the ordinary space, while the higher negative moments about the outer part of the jet. In addition to the moments, we take three more measures; a) the ratio of the electromagnetic (EM) calorimeter response to the total (EM+HAD) calorimeter response (EM/TOTAL), b) the "asymmetry" and c) the "oblateness" of a jet. The asymmetry and the oblateness are measures about the non-uniform momentum distribution with respect to the jet axis. For each jet, we calculate a tensor, $T_{x'x'} = \sum_{i=1}^{n} p_{ix'}^2$, $T_{x'y'} = T_{y'x'} = \sum_{i=1}^{n} p_{ix'}p_{iy'}$, and $T_{y'y'} = \sum_{i=1}^{n} p_{iy'}^2$, where the axes x' and y' are in the plane perpendicular to the jet axis (z'-axis). The asymmetry is defined as $A = (T_{y'y'} - T_{x'x'})/(T_{y'y'} + T_{x'x'})$, where the x' axis is in the jet production plane and the y' axis is in the direction perpendicular to it. The oblateness O is defined by eigenvalues d_1 and d_2 ($d_1 > d_2$) of the T-tensor as $O = (d_1 - d_2)/(d_1 + d_2)$.

Figures 1a), b) and c) show several distributions of the mechanical moments for the MC and CDF jets for the E_t range of 30−40 GeV in the logarithmic scale. These moments are calculated from the transverse/longitudinal components of particle momenta. Both distributions for the reference (MC) and the real (CDF) data are normalized so that the integrations of the distributions over the entire moment range are unity: $\int P_q(x)dx = \int P_g(x)dx = \int P_r(x)dx = 1$, where $P_q(x)$, $P_g(x)$ and $P_r(x)$ are distributions of a moment x for quark,gluon samples and real data, respectively.

First, we will discuss the results on the MC jets. As an example of the moment distributions, we present those of the moment $(P_t/M)^{-3}$ for MC quark and gluon jets in fig. 1a. In this figure, gluon distributions peak at a larger value of the moment than the quark distributions. The other distributions of the transverse negative power moments, which are not presented, show similar trends. It implies that the gluon jets are "broader" than the quark jet. The longitudinal moments $(P_l/M)^{-1}$ and $(P_l/M)^3$ are also shown in fig. 1b and c, respectively. In these figures, the quark jets have larger values of the positive power moments, and lower values of the negative power moments than gluon jets. This means that fragments of quark jets are "harder" than those of gluon jets. Finally in fig. 2b), we show the EM fraction of jets. We see that the gluon jet has a larger EM fraction than the quark jet: Fragments of gluon jet have more chances to shower in the EM calorimeter. The EM fraction increases with number of produced π^0's in a jet. The gluon may produce more π^0's than the quark because of its neutral charge, and consequently may get a large EM fraction.

Summarizing the results of figs. 1 and 2 about the MC events, we conclude that gluon jets are broader and contain more soft particles than quark jets: Hadrons from a quark are harder and more collimated than those from a gluon. The discrepancies between the two MC generators are small, namely, both fragmentation models give similar predictions. This is understandable, because they are based on the same color-flow scheme.

Next, we will compare the moment distributions for the CDF and MC jets. The results for the CDF jets are also presented in figs. 1 and 2. In figs. 1a),b),c), we observe that the moment distributions for the CDF jets are generally close to those for gluon jets. The distribution of the EM fraction and the multiplicity of the real data are also close to those of the gluon jets as shown in figs. 2a) and b). However, if one takes a closer look at the moment distributions of the CDF dijets, one notes discrepancies between theory and the CDF results. According to the QCD prediction, the CDF dijet sample should contain approximately 20% of the quark jet fraction at low E_t (10 GeV) and 30% at high E_t (50 GeV). One thus expects the moment variables for the CDF dijets distribute between those for the quark and the gluon MC references. The moment distributions for the CDF dijets, however, show that they are even softer and broader than the MC gluon jets. In

addition, as shown in figs. 3a), b), and c), this tendency is standing out at lower E_t. We hence conclude that real gluon-initiated jets are softer and broader than those predicted by the current fragmentation models

Although there exist some discrepancies between the MC and the real jets as discussed above, we use in the present analysis the current fragmentation models for the quark-gluon separation. We propose a statistical approach which characterizes each jet in a certain single measure. First, a quark vs. gluon likelihood is calculated from single variable distributions as follows. Let us denote the i-th moment by x_i (i = 1,2,...,n), and its distributions for quark and gluon sets by $P_q(x_i)$ and $P_g(x_i)$, respectively. A measure of the degree with which a jet with a moment x_i is more likely from a quark than from a gluon is the log-likelihood $L_i(x_i)$, defined by

$$L_i(x_i) = \ln\left[\frac{P_q^{(i)}(x_i)}{P_g^{(i)}(x_i)}\right] , \tag{1}$$

where the integrations of the distribution functions over x_i's are normalized to unity. The next question is how to integrate the information on the likelihood L_i's obtained from individual moments to get a "global" likelihood. If the moments x_i's are mutually independent, the global likelihood is a simple sum of L_i's. The distributions of moments are actually not independent. For simplicity of the treatment, we shall here take an equal-weighted sum, but also introduce one scale parameter to represent the effect of correlations among variables. Thus in the present analysis, the global likelihood is defined by

$$L' = \lambda \sum_{i=1}^{n} L_i = \lambda L , \tag{2}$$

where λ is a scale parameter. We will denote the difference of means of L (L') for quark and gluon reference jets by Δ (Δ'), and the combined deviation for the two references by σ (σ'). As shown in Appendix A, if the global likelihood distributions are symmetric Gaussian functions, L' is the proper likelihood with a scale factor:

$$\lambda = \frac{\Delta}{\sigma^2} . \tag{3}$$

The figure of merit or the separation power of the global likelihood can be defined as

$$S = \frac{\Delta'}{\sigma'} , \tag{4}$$

which is equal to σ' for the proper likelihood.

Let us next consider the errors of the likelihood. The errors of individual likelihood, σ_{Li}'s, are in general mutually correlated, but we assume that the effect

is again represented by the scale factor λ, and that the uncertainty of the global likelihood, $\sigma_{L'}$, is given by

$$\sigma_{L'} = \lambda\sqrt{\sum \sigma_{Li}^2}\,. \tag{5}$$

The likelihood L_i is evaluated from the distribution functions $P_q(x_i)$ and $P_g(x_i)$ by eq. (1), hence its error is given by

$$\sigma_{Li} = \sqrt{\left(\frac{\sigma_q}{P_q}\right)^2 + \left(\frac{\sigma_g}{P_g}\right)^2 + \left(\frac{1}{P_q}\cdot\frac{\partial P_q}{\partial x_i} - \frac{1}{P_g}\cdot\frac{\partial P_g}{\partial x_i}\right)^2 \sigma_{xi}^2}\,. \tag{6}$$

There are several sources of systematic uncertainties which contribute to σ_{Li}, in particular when we deal with real data provided by experiments. The uncertainties are of two kinds: One is that of the distribution functions themselves due to our imperfect knowledge of the fragmentation. The other is the error in the experimental determination of x_i, which is a combination of systematic effects due to clustering, and detector originated uncertainties such as low energy calorimeter responses, calibration systematic errors, finite detector resolution and simulation uncertainties. We however do not assign here the errors from these sources to σ_{Li}, just for simplicity. Note that the σ_{xi}^2 term in eq (6) has a coefficient which is small when the P_q and P_g are nearly equal as in the present case. Thus, we ignore the third term on the right hand side of eq. (6), and take only the statistical errors for σ_g and σ_q, which are due to the finite number of events in a given x_i-bin in the reference data sets.

In the actual analysis described in this paper, the histogram of each moment was divided into 50 bins, and the total binwidth was chosen wide enough. The statistical errors, σ_q and σ_g, are assigned to each bin, assuming a Gaussian fluctuation. It is to be noted that this kind of statistical error can be reduced as much as one likes by accumulating the reference jet data.

Finally, we take eq. (5) as the error of L' for a jet, and make a smoothing of the L' distribution, supposing that L' is distributed with a Gaussian function with uncertainty $\sigma_{L'}$.

Before discussing the results on the global likelihood, we will review the discriminating powers of individual moments. To quantify them, we use the figure of merit defined by $s_i = \frac{\Delta_i}{\sigma_i}$. Fig. 4 shows the figures of merit for 30 variables Assignments of variable numbers to moments are listed in Table 1. We note that some variables, for instance, the multiplicity and a moment $\sum(P_{cli}/M)^3$, have rather large figures of merit. Also,the results from two MC generators show fairly good agreements, except that for "transverse" moments Pythia predicts relatively larger figures of merit than Herwig.

The resulting global likelihood shows different normalized distributions $Q(L')$ for quarks and $G(L')$ for gluons as presented in figs. 5a) and b). In these figures, the

global likelihood distributions for the CDF dijet and γ+jet events are also shown. When given a data set to analyze, which we will call an "analysis" sample, we can determine a quark vs. gluon likelihood for each jet in the sample. By cutting jets below a certain level of the likelihood L'_c, we can enhance the quark-to-gluon ratio and obtain a signal-richer sample accordingly. The signal-to-background ratio is then given by

$$r = \frac{N_q \int_{L'_c}^{\infty} Q(L')dL'}{N_g \int_{L'_c}^{\infty} G(L')dL'}, \tag{7}$$

where N_q and N_g are numbers of jets in the original analysis sample respectively.

We can also determine the fraction of the gluon (or quark) jets in a given analysis sample without any cut. The predictions from two references are fit to the analysis sample in a form:

$$D_i = X_g G_i + (1 - X_g) Q_i \tag{8}$$

by finding the coefficient X_g which minimizes the chi-squared defined by

$$\chi^2 = \sum_{i=1}^{50} \left[\frac{D_i - (X_g G_i + (1 - X_g) Q_i)}{\sigma_i} \right]^2 . \tag{9}$$

In eqs. (8) and (9), G_i, Q_i, and D_i are (normalized) numbers of jets in the i-th bin of the likelihood histograms for gluon, quark, and analysis samples respectively; σ_i is an error on D_i: $\sqrt{D_i}$.

In fig. 6, we plot the fraction of the final state gluon in the CDF dijet events, γ+jet events, and π^0+jet events as a function of jet transverse energy E_t. The π^0 candidates are selected with the same cuts those for photon candidates, except the strip χ^2_{av} cut, i.e., the χ^2_{av} is required to be greater than 5. As usual, the errors on the gluon fraction are given by the set of $X_g^{(-)}$ and $X_g^{(+)}$ such that $\chi^2(X_g^{(-)}) = \chi^2(X_g^{(+)}) = \chi^2_{min}+1$. The figure shows that dijet data contain approximately 80% of gluon fraction in the jet transverse energy (E_t) range of 10−30 GeV, and reproduce qualitatively the expected E_t dependence of the gluon fraction, i.e. the fraction gradually decrease with E_t. However, this tendency appears more strongly on real data than MC data. The difference is consistent with the results on the moment distributions that the CDF dijets are softer and broader than the MC gluon jets, a trend which enhances at lower values of E_t. The γ_{cand}+jet data contain about 40% gluon fraction in E_t range of 10−30 GeV. These results agree within the error with the gluon fraction determined from theoretical prediction and the expected π^0/γ ratio in the photon candidates. In addition, π^0+jet data agree quite well with the MC simulation of the QCD process, in which very hard π^0's (with momentum fraction $z > 0.7$, 0.8) are assumed to be generated.

We acknowledge the vital contributions of the members of the Fermilab accelerator division and the technical staffs of the participating institutions. This work

was supported by the U.S. Department of Energy, the National Science Foundation, the Italian Istituto Nazionale di Fisica Nucleare, the Ministry of Science, Culture and Education of Japan, and the A. P. Sloan Foundation.

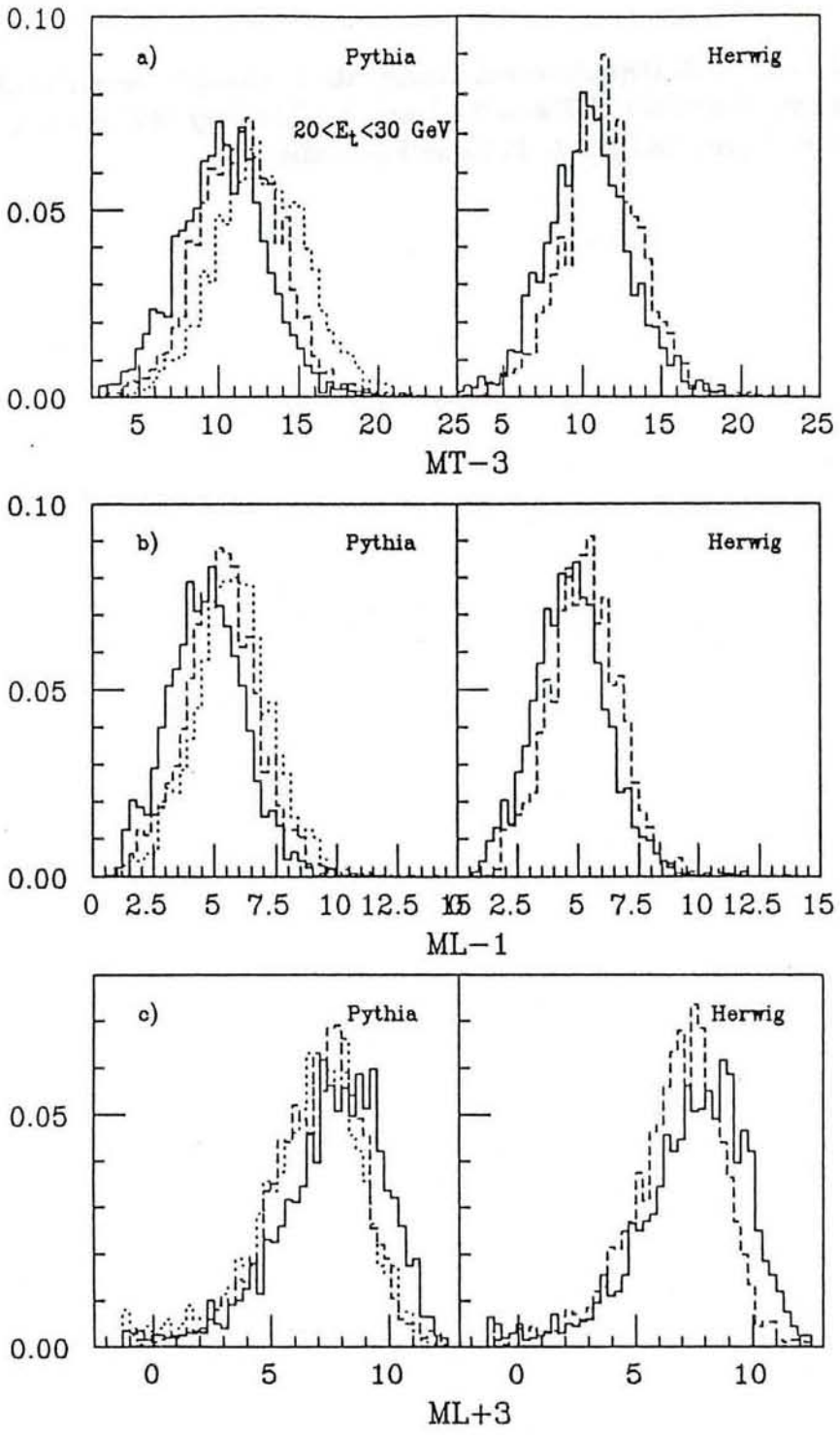

Figure 1: Distribution of moments: a) $\ln|\sum(p_{ti}/M)^{-3}|$, b) $\ln|\sum(p_{ti}/M)^{-1}|$, and c) $\ln|\sum(p_{ti}/M)^{3}|$, where the sum is over charged tracks associated with a jet; $P_t(P_t)$ is the track longitudinal(transverse) momentum with respect to the jet axis, and M is the jet invariant mass. Solid histogram: quark jets. Dashed: gluon jets. Dotted: CDF dijet data. The E_t range of jets is 30−40 GeV. The quark and gluon jets were produced with Herwig/Pythia and a detector simulation.

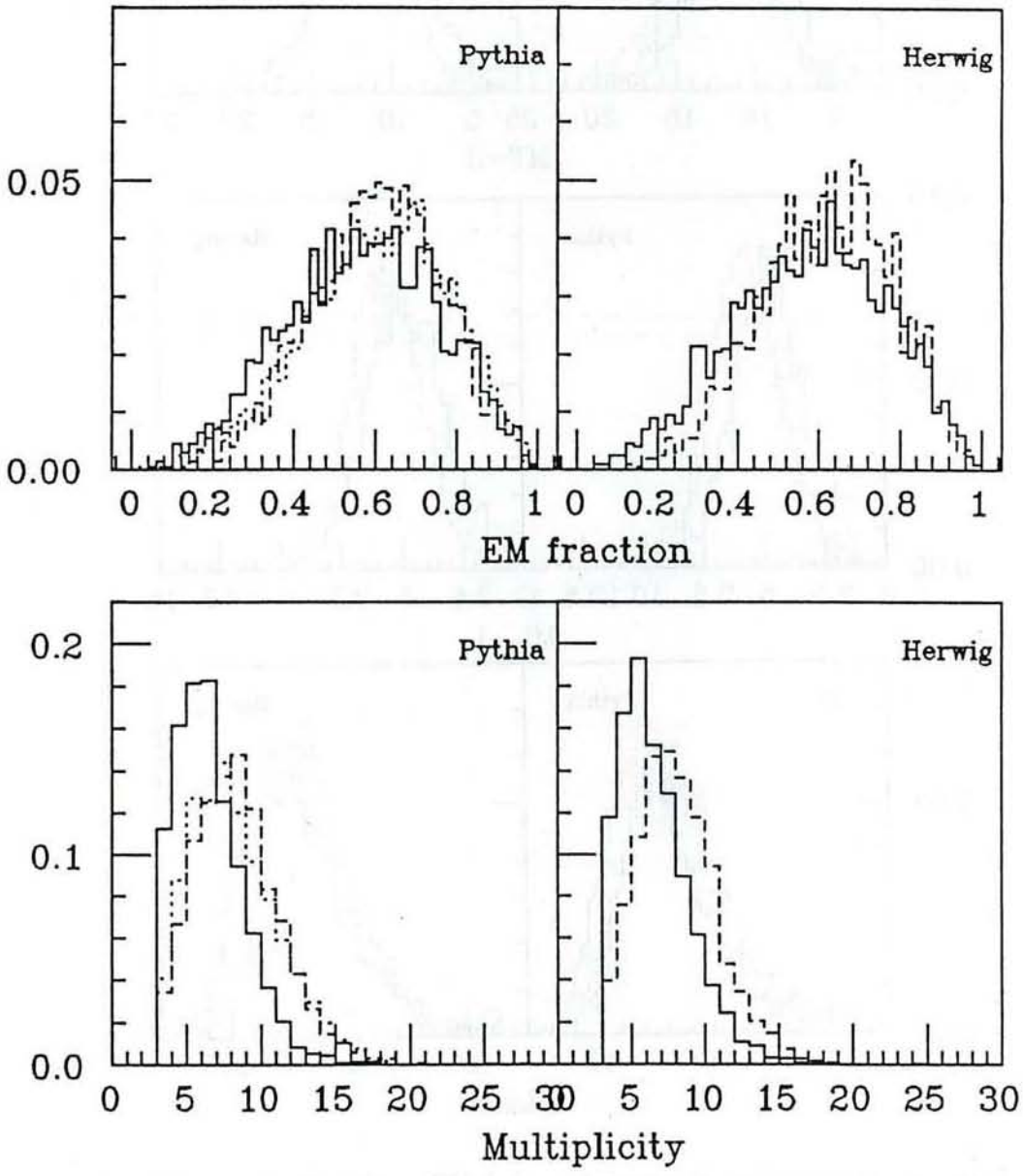

Figure 2: Distributions of jet charged multiplicity and EM energy fraction of the jet. Solid histogram: quark jets. Dashed: gluon jets. The E_t range of jets is 30–40 GeV.

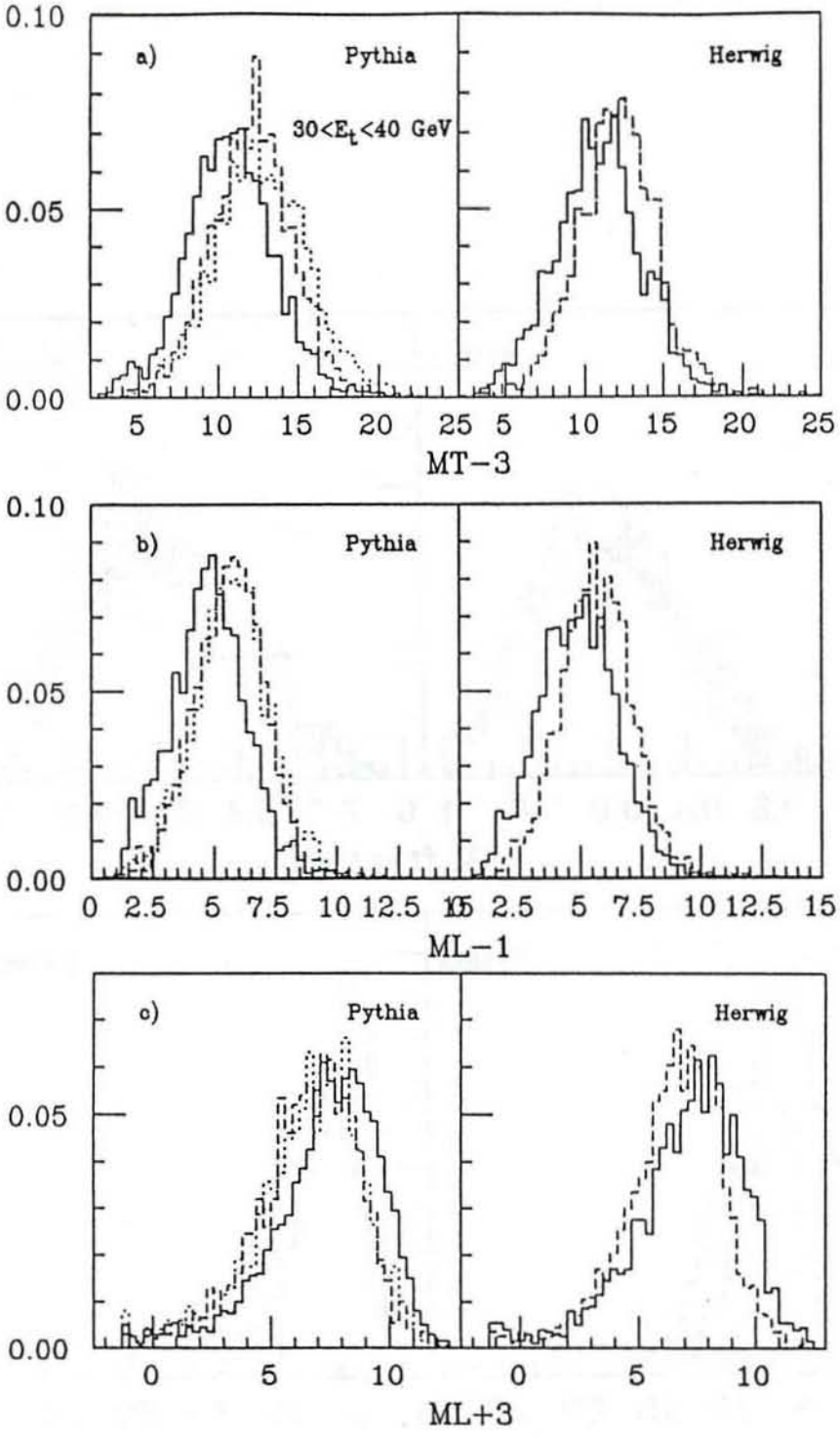

Figure 3: Distribution of moments: a) $\ln|\sum(p_{ti}/M)^{-3}|$, b) $\ln|\sum(p_{ti}/M)^{-1}|$, and c) $\ln|\sum(p_{ti}/M)^{3}|$. Solid histogram: quark jets. Dashed: gluon jets. Dotted: CDF dijet data. The E_t range of jets is 20−30 GeV. The quark and gluon jets were produced with Herwig/Pythia and a detector simulation.

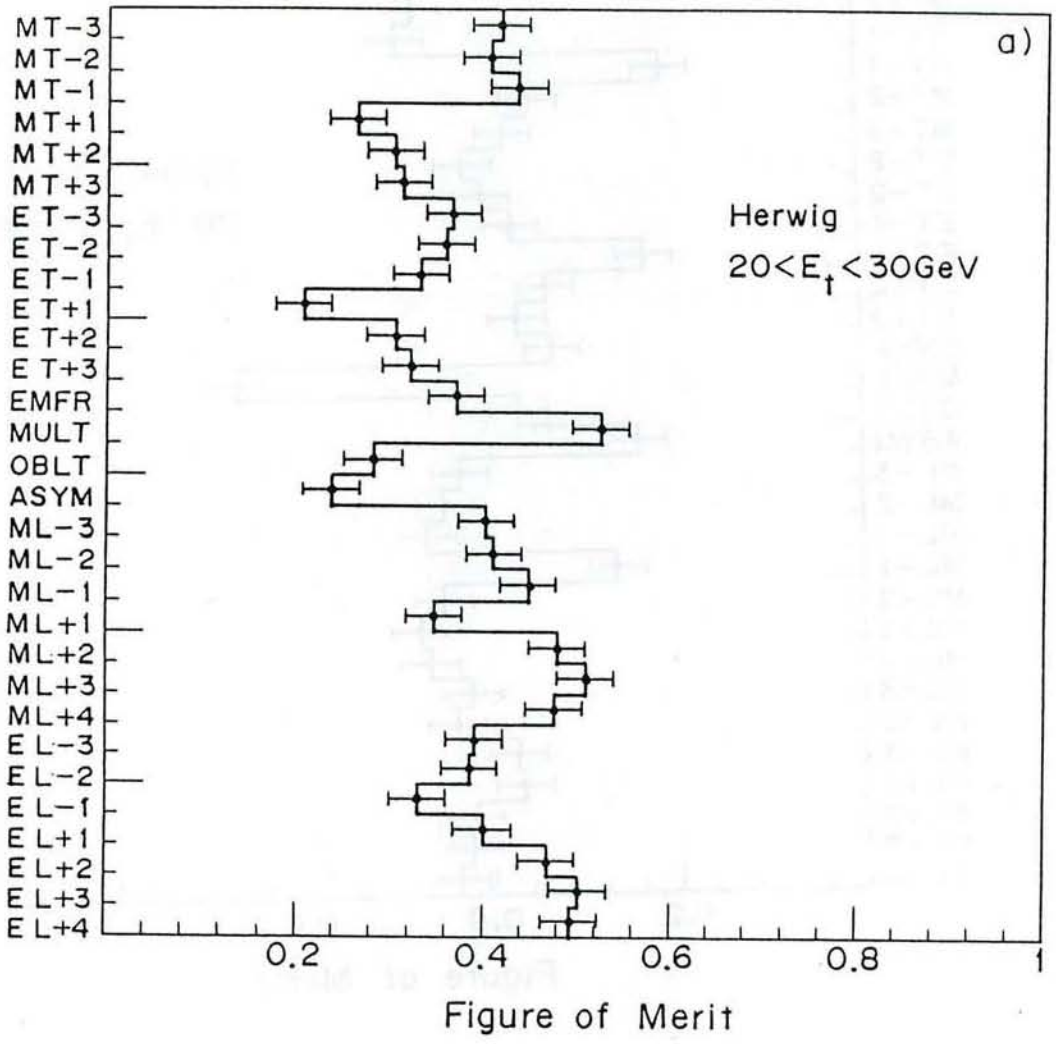

Figure 4: Figures of merit of 30 variables for two Monte Carlo generators: a) Herwig and b) Pythia. The letters, MT, ET, ML and EL followed by positive/negative numbers (the power of moment) mean "Mechanical Transverse moment", "Electrical Transverse moment", "Mechanical Longitudinal moment" and "Electrical Longitudinal moment", respectively (see Table 1). The other four letters, EMFR, MULT, OBLT and ASYM refer to the electro magnetic fraction of a jet, charged multiplicity within a jet, oblateness of jet and asymmetry of jet fragments, respectively. The data points were shown for the sample of simulated jets with transverse energy E_t 20−30GeV, with their statistical errors

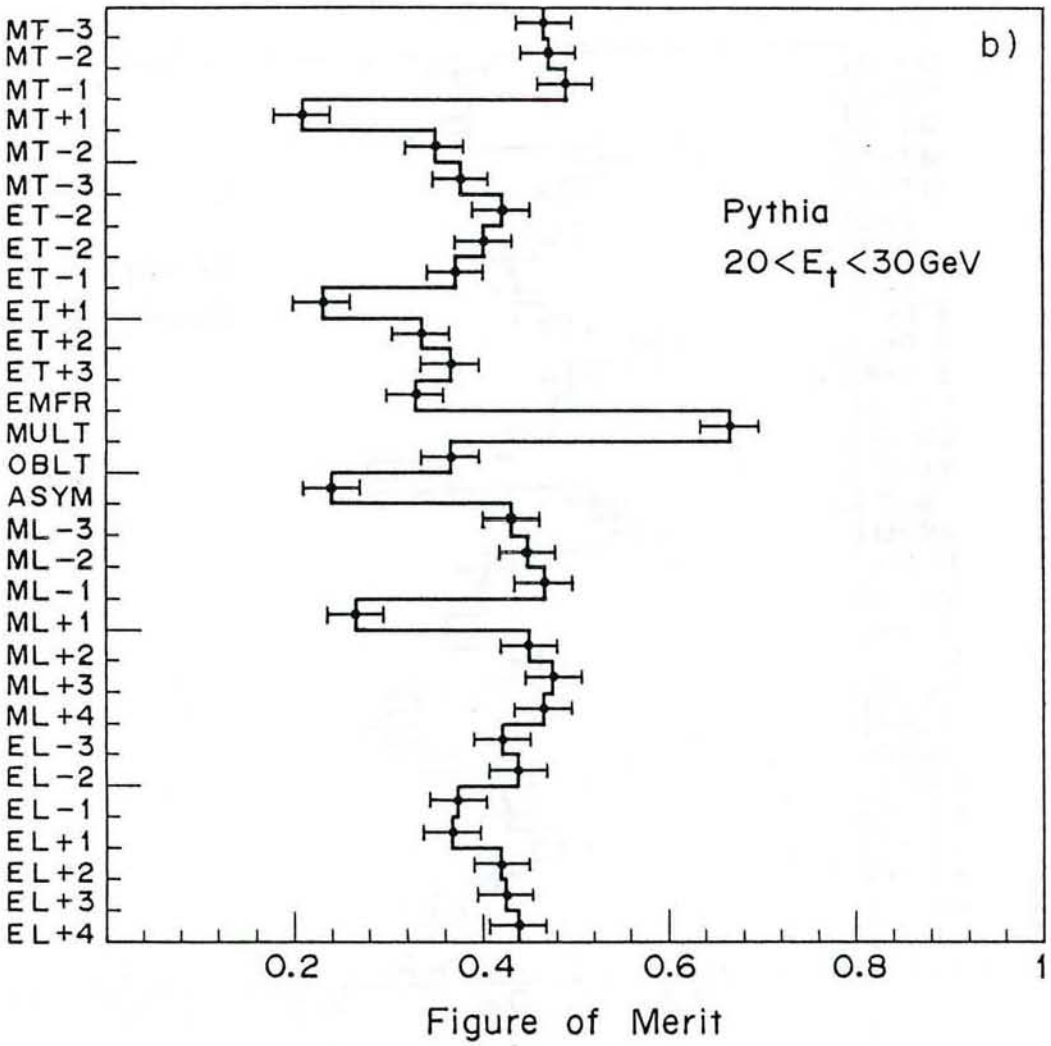
MT-3
MT-2
MT-1
MT+1
MT-2
MT-3
ET-2
ET-2
ET-1
ET+1
ET+2
ET+3
EMFR
MULT
OBLT
ASYM
ML-3
ML-2
ML-1
ML+1
ML+2
ML+3
ML+4
EL-3
EL-2
EL-1
EL+1
EL+2
EL+3
EL+4
b)
Pythia
20<E_t<30GeV
0.2
0.4
0.6
0.8
1
Figure of Merit

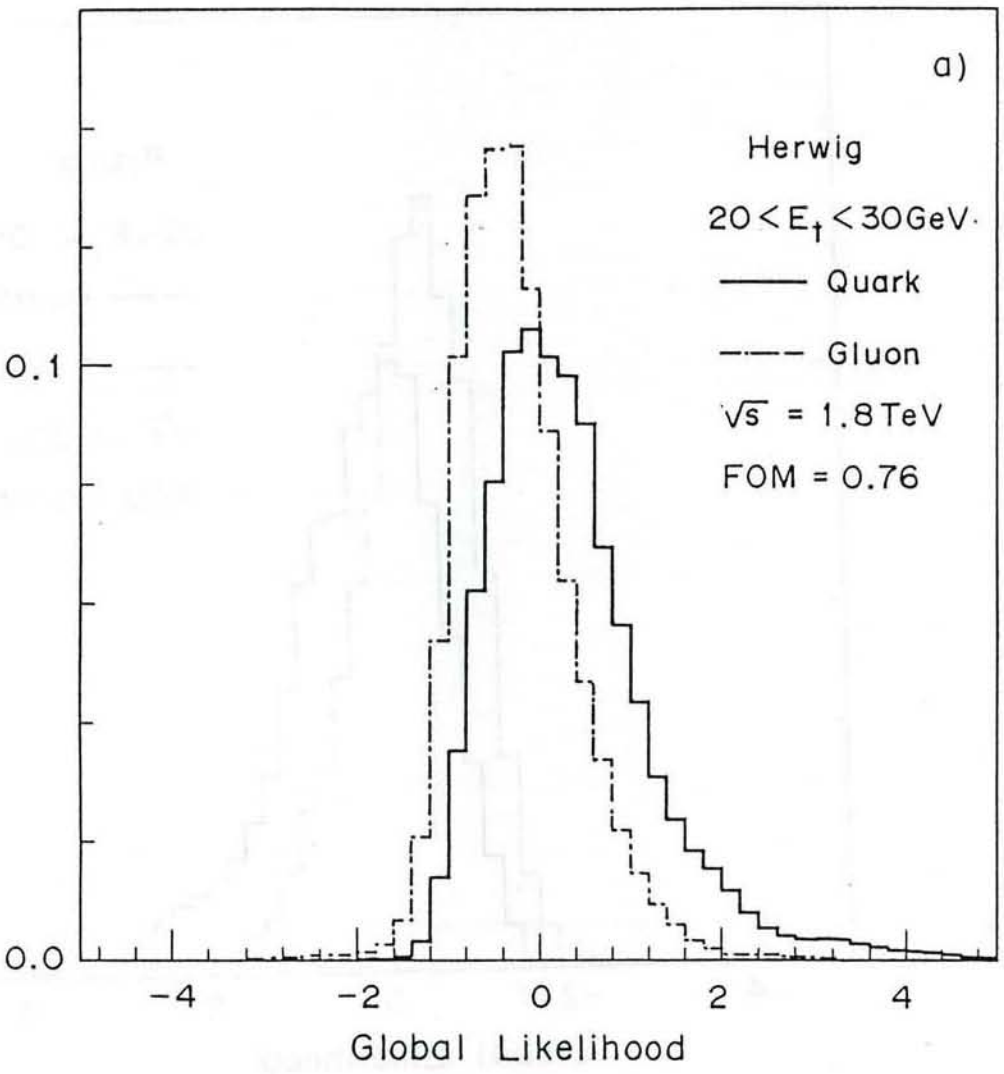

Figure 5: Distribution of "global likelihood" for the samples generated with a) Herwig and b) Pythia in $\bar{p}p$ collisions at $\sqrt{s}$=1.8 TeV. The both generated quark and gluon jets were processed through the detector simulation, and then reconstructed with a cone algorithm. The E_t range of the sample is 20−30GeV.

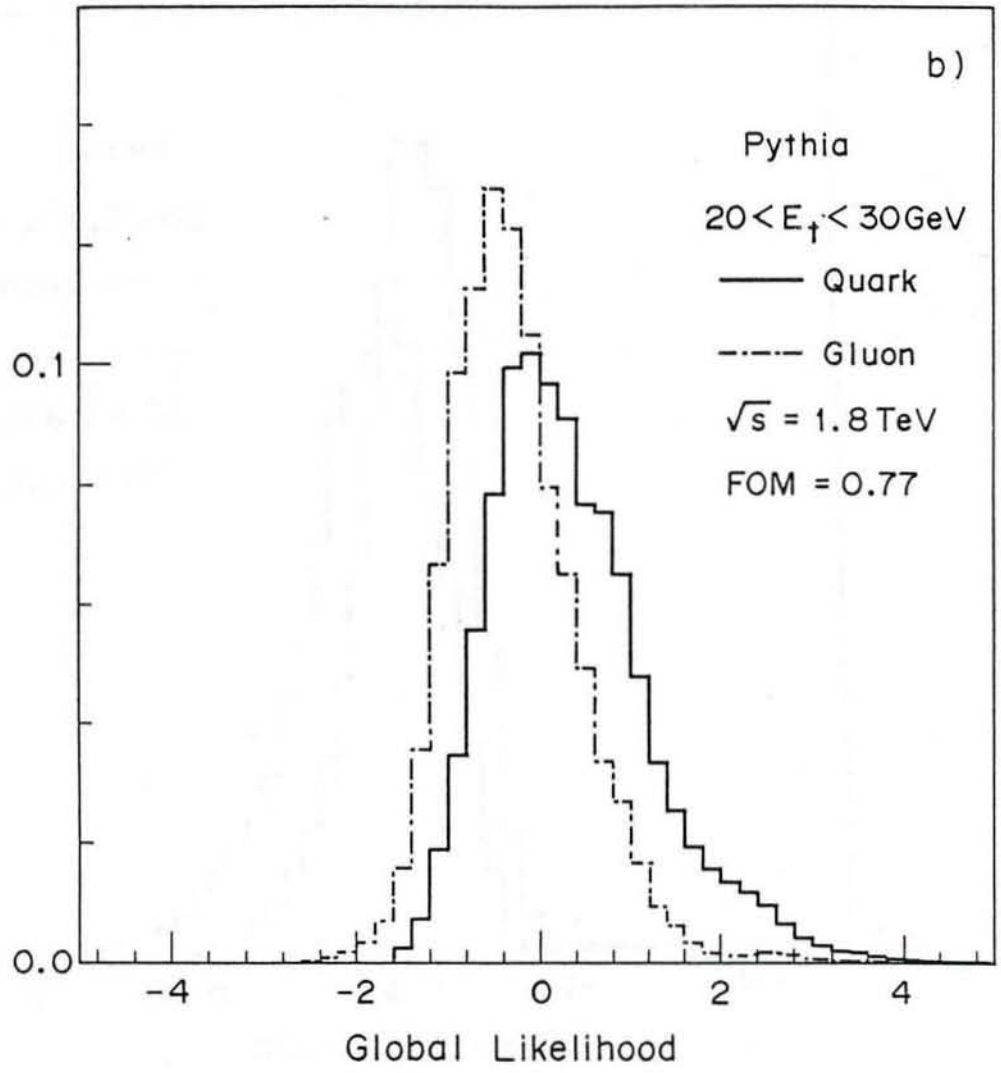
b)
Pythia
20 < E_t < 30 GeV
Quark
Gluon
√s = 1.8 TeV
FOM = 0.77
0.1
0.0
-4
-2
0
2
4
Global Likelihood

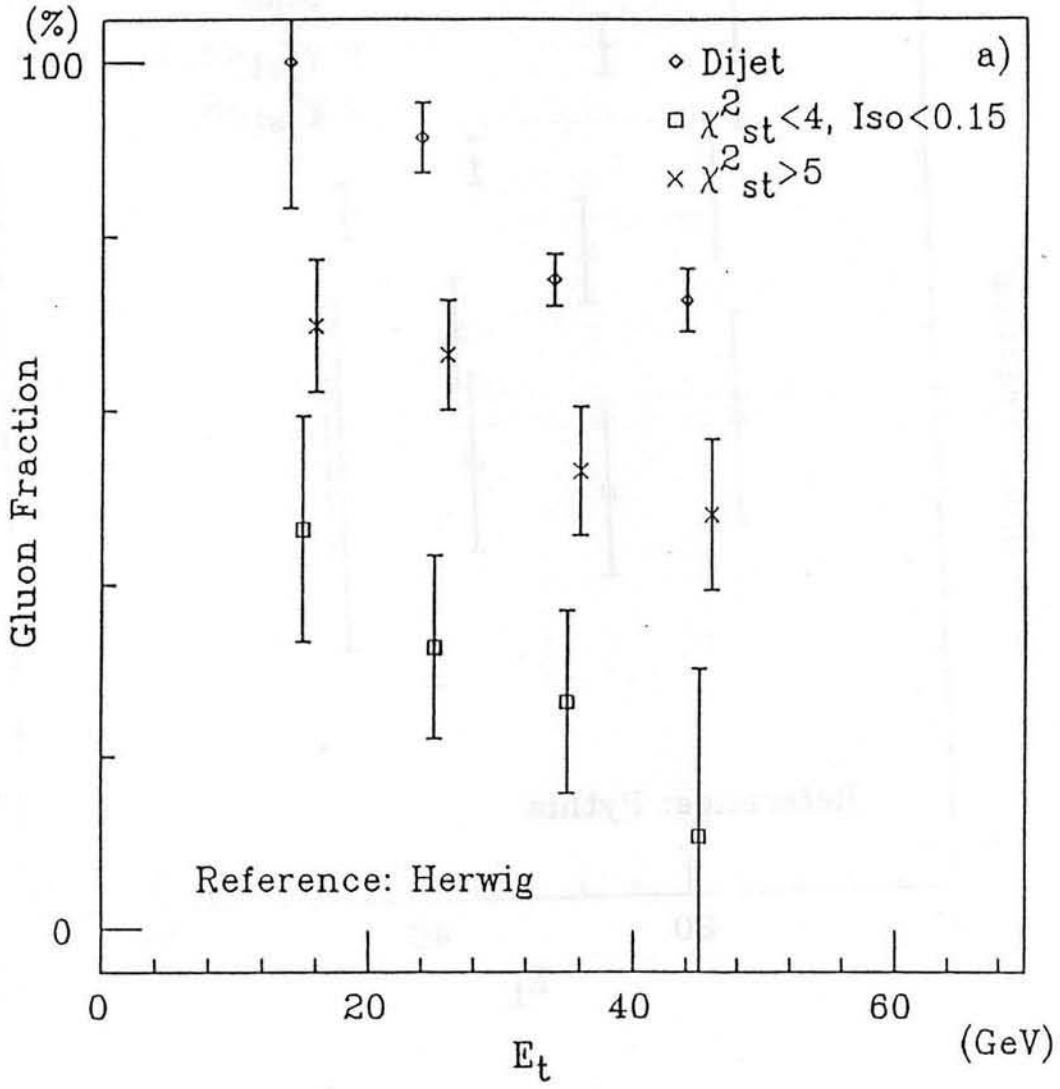

Figure 6: The fraction of the final state gluon in the dijet events from 1987 run, γ+jet events from 1988−89 runs, and π^0+jet events sample, as a function of jet transverse energy E_t. The calculation of the fraction has been carried out using QCD Monte Carlo data as reference quark and gluon jets, which were generated with Herwig and Pythia, and simulated with a detector simulation QFL.

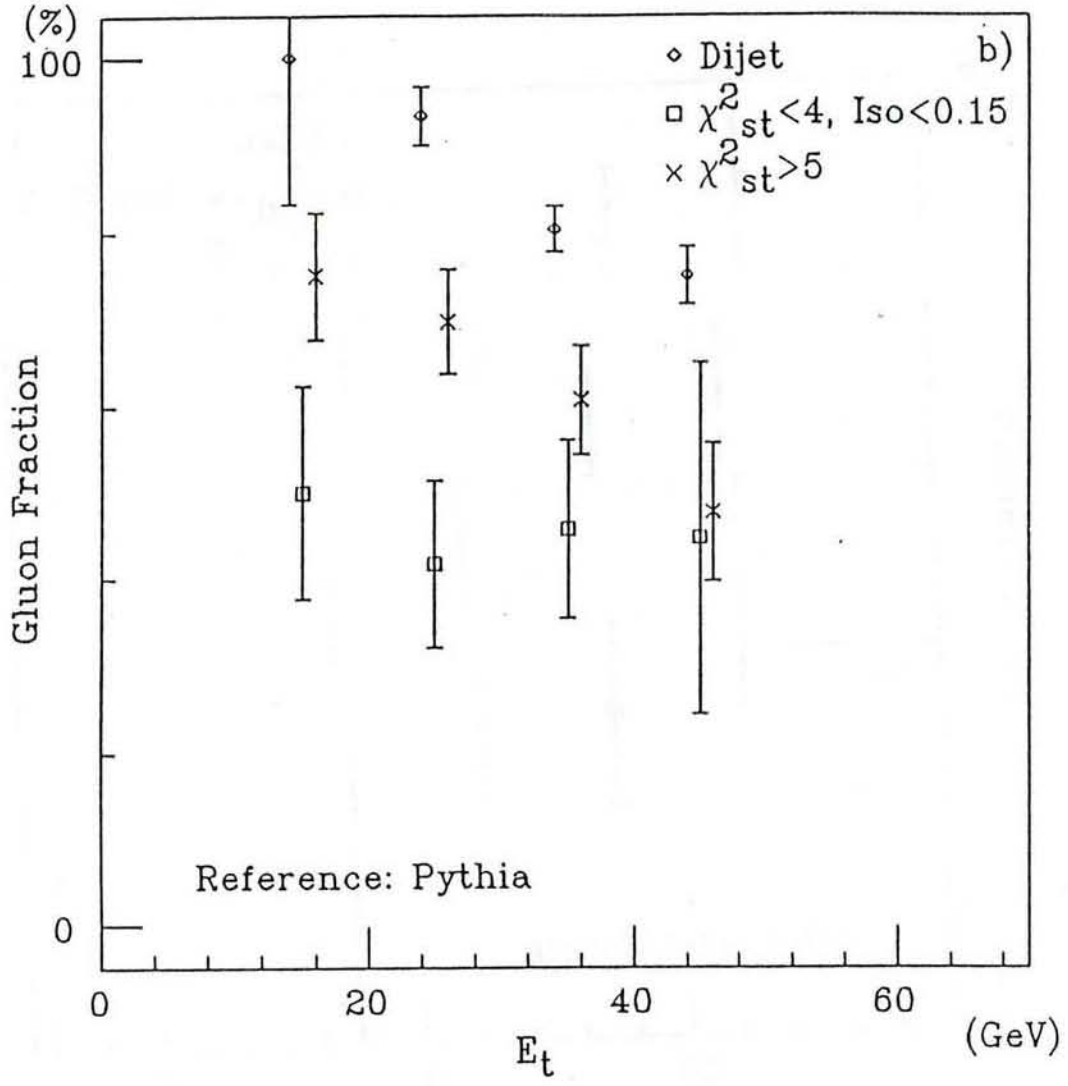
(%)
100
0
Gluon Fraction
◇ Dijet
b)
□ χ^2_{st}<4, Iso<0.15
× χ^2_{st}>5
Reference: Pythia
0
20
40
60
E_t
(GeV)

Appendix A

Gaussian likelihood distributions

The procedure to find a global likelihood from multi-dimensional likelihood functions is not unique. In this appendix, we point out a general relation which the properly defined likelihood should satisfy, and discuss a simple case where the likelihood distributions for two reference samples are Gaussian functions.

If a parameter L' is a properly defined likelihood, a relation for L',

$$L' = \ln\left[\frac{Q(L')}{G(L')}\right], \tag{A.1}$$

or, equivalently, a relation for the quark fraction f_q,

$$f_q = \frac{Q(L')}{Q(L') + G(L')} = \frac{1}{1+\exp^{-L'}} \tag{A.2}$$

should hold. In eqs. (A.1) and (A.2), $Q(L')$ and $G(L')$ are likelihood distributions for the quark and gluon samples.

If one assumes that L is a certain parameter representing a measure of likelihood, and that $Q(L)$ and $G(L)$ are Gaussian functions with means μ_q and μ_g and variances σ_q and σ_g, respectively, then it is easy to show that the condition (A.1) requires

$$\mu_q = -\mu_g(=\mu),\ \sigma_q = \sigma_g(=\sigma), \tag{A.3}$$

and

$$\Delta/\sigma^2 = 1\,, \tag{A.4}$$

where $\Delta = \mu_q - \mu_g = 2\mu$.

Suppose one found a parameter L whose distributions are Gaussian functions which satisfy eqs. (A.3). Then the condition (A.4) can be satisfied by a scale transformation,

$$L \to \lambda L = L',\ \mu \to \lambda\mu = \mu',\ \sigma \to \lambda\sigma = \sigma',\ \Delta \to \lambda\Delta = \Delta' \tag{A.5}$$

with $\lambda = \Delta/\sigma^2$. The separation power for such samples is given by a simple parameter σ' as

$$S = \frac{\Delta'}{\sigma'} = \frac{\Delta}{\sigma} = \sigma'\,. \tag{A.6}$$

References

[1] P. Ghez and G. Ingelman, DESY preprint DESY 86-110 (1986);
G. Arnison et al., Nucl. Phys. B276 (1986) 253

[2] W. Bartel et al., Phys. Lett. 123B (1983) 460

[3] A. Petersen et al., Phys. Rev. Lett. 55 (1985) 1954

[4] M. Derrick et al., Phys. Lett. 165B (1985) 449

[5] Y.K. Kim et. al., KEK preprint 89-44 (1989)

[6] L.M. Jones, Tsukuba preprint UTHEP-189 (1989)

[7] R.D. Field and R.P. Feynman, Nucl. Phys. B136 (1978) 1

[8] B. Andersson, G. Gustafson and C. Peterson, Z. Phys. C1 (1979) 105;
B. Andersson, G. Gustafson and B. Söderberg, Z. Phys. C20 (1983) 317

[9] S. Wolfram, in Proc. 15th Rencontre de Moriond (1980), ed. J.Tran Thanh Van;
G.C. Fox and S. Wolfram, Nucl. Phys. B168 (1980) 285;
R.D. Field and S. Wolfram, Nucl. Phys. B213 (1983) 65

[10] T.D. Gottschalk, Nucl. Phys. B214 (1983) 201; B227 (1983) 413;
T.D. Gottschalk, in Proc. UCLA workshop on SSC physiscs (1986)

[11] G. Marchesini and B.R. Webber, Nucl. Phys. B238 (1984) 1;
B.R. Webber, Nucl. Phys. B238 (1984) 492

[12] M.D. Corcoran, Phys. Rev. D32 (1985) 592;
M.W. Arenton et al.(E609), Phys. Rev. D31 (1985) 984

[13] C.de Marzo et al.(NA5), Nucl. Phys. B211 (1983) 375; B234 (1984) 1

[14] B.R. Webber, Cavendish-HEP-88/6, August 1988;
B.R. Webber, Phys. Lett. 193B (1987) 91

[15] H.-U. Bengtsson and T. Sjöstrand, Computer Phys. Comm. 46 (1987) 43

[16] T. Sjöstrand , Computer Phys. Comm. 39 (1986) 347;
T. Sjöstrand and M. Bengtsson, Computer Phys. Comm. 43 (1987) 367

[17] F. Abe et al., Nucl. Instr. and Meth. A271 (1988) 387

[18] F. Abe et al., Phys. Rev. Lett. 62 (1989) 613

[19] A. Byon and A. Para, CDF Note No.570; No.571